Presentation 2

LEP Magnetic Field Defects

By J.P. Gourber

2.1 Summary

This note summarises the imperfections of the magnetic fields which are seen by the beams and which thus include the contributions of the magnets themselves, of their alignment and of their environment (vacuum chambers and proximity effects). The results are given for the dipole chain, the regular lattice quadrupoles and the sextupoles and in a global way for the dispersion region and straight section quadrupoles. The figures compiled in this note have been provided mainly by J. Billan and K.N. Henrichsen for the dipoles [1], V. Remondino, R. Wolf and C. Wyss for the lattice magnets [2], as well as by M. Hublin and M. Mayoud for the alignment. Some parameters which are still under investigation are missing; they will be settled in a more complete LEP Note to be issued on the same subject.

2.2 Dipole chain

Tables 2.1, 2.2 and 2.3 give the systematic and random field errors for the main dipoles, the low field dipoles and the returned dipoles (half cells 136 and 164 respectively). The vertical (or normal) and horizontal(or skew) fields in the median plane integrated over a dipole pair are developed in multipoles

$$B_y = B_0\left(a_1 + a_2 x + a_3 x^2 + a_4 x^3 .....\right) \quad (2.1)$$

$$B_x = B_0\left(b_1 + b_2 x + b_3 x^2 + b_4 x^3 .....\right) \quad (2.2)$$

and for each multipole, the error is given as the corresponding integrated field error at the aperture of 0.059m:

$$\frac{\Delta B_y l_{(x=0.059m)}}{B_y l_{(x=0)}} \quad \text{or} \quad \frac{\Delta B_x l_{(x=0.059m)}}{B_y l_{(x=0)}}$$

In the case of the main dipoles, an "average pair" having a field integral equal to 1/3 of that of a B6 half-cell has been considered. For the low field dipoles (Table 2.2) the errors are referred to the integrated field $B_y l_{(x=0)}$ of a pair of main dipoles; in such a case the perturbation of the

vacuum chamber is the same as for the main dipole (the nickel layer at full saturation giving a constant ΔBl at all field levels).

The r.m.s. errors of the magnet themselves are deduced from the magnetic measurements; those introduced by the vacuum chamber have been calculated from the systematic errors assuming a proportionality to the nickel thickness and a r.m.s. dispersion of 9% of the latter (as measured on about 30 chambers by J. Billan). The alignment errors only contribute to the vertical and horizontal field dispersion via the length of the pairs ($< \Delta l/l > = 1.5\ 10^{-4}$ r.m.s) and the transverse tilt ($< \Delta\theta >= 10^{-4}$ rad r.m.s) respectively.

In the case of the skew field, only the dipole component has been measured on each individual core; the skew quadrupole and sextupole errors quoted in Tables 2.1 to 2.3 are linked to the errors in the position of the excitation bars and those quoted for the vacuum chambers have been deduced from coupling measurements (see below).

The field errors quoted in the Tables have a limited precision; this is particularly evident for the systematic errors ϵ introduced by the vacuum chamber which have been measured on one sample only selected so as to have roughly the average thickness of the nickel layer; it is also true for the field errors ϵ of the magnet themselves which include several corrections (fit used to deduce the multipoles, geometry of the measuring coil, end effects, core aging). The precision on the various multipoles will be given in the future LEP Note. Today it is reasonable to assume a precision of the order of $\pm 10^{-4}$ on the systematic errors ϵ for the magnets and vacuum chamber and ± 2 10^{-4} for the global errors; this means that the discrepancy quoted by A. Verdier between the LEP model at 20 GeV (based on the values of Tables 2.1 to 2.3) and the beam parameters can be **fully explained for the tunes** (+10% increase of the quadrupole term in the main dipoles) and **partially explained for the chromaticity** (a factor 4 increase of the sextupole term in the dipoles giving $-3 \cdot 10^{-4}$ instead of $-0.8 \cdot 10^{-4}$ is possible, and close to the factor 6 quoted by A. Verdier).

It should also be noted that the field errors are well within the tolerances set for the LEP project [3] with the exception of the systematic quadrupole of the main dipoles which is marginally out at 20GeV.

2.3 Injection region dipoles

The field errors of Table 2.4 are quoted for single 5.75m. long magnets and are referred to their actual field integral (twice the main bending field). The dipole dispersion $< \Delta e >$ takes into account the mixing of magnets according to their actual field integrals. The errors due to the vacuum chambers are reduced with respect to the main dipoles by a factor 2 for the systematic values (field ratio) and only by $\sqrt{2}$ for the random values ($\sqrt{2}$ increased Ni thickness dispersion due to shorter lengths).

As for the main dipoles, the systematic and random errors are well within tolerances.

2.4 Regular lattice quadrupoles QF and QD

Table 2.5 gives the gradient errors at 20GeV and 45GeV before the β-squeezing; for each component, the quoted value is the corresponding error on the gradient integral in the median plane at the aperture limit of 0.059 m:

$$\frac{\Delta(\partial B_x l/\partial x)_{x=0.059m}}{\partial B_y l/\partial x_{x=0}} \quad \text{or} \quad \frac{\Delta(\partial B_y l/\partial x)_{x=0.059m}}{\partial B_y l/\partial x_{x=0}}$$

The perturbation of the quadrupole field due to the nearby sextupole and corrector has been measured and incorporated into the columns "magnet", the only visible effect is a reduction of the

normal octupole component of 5.0 10^{-4} at 20GeV and 1.8 10^{-4} at 45GeV due to the sextupole. The r.m.s. values quoted for the vacuum chamber have been calculated for a dispersion of 11% r.m.s. of the thickness of the nickel layer (as measured on 21 vacuum chambers) assuming a proportionality to the thickness.

The reduction of the quadrupole strength introduced by the vacuum chamber has been taken into account in the Gl/I tables used for LEP operation. The normal octupole (33.1 10^{-4}) and dodecapole (-39.9 10^{-4}) at 20 GeV, which are essentially due to the vacuum chamber, appear quite large and exceed the tolerances specified (5 10^{-4} and 10^{-3} respectively). However if in a first approximation we ignore the azimuthal variation of β and η and simply calculate the corresponding field integral errors in the half cell we obtain:

$$\frac{\Delta(B_y l)_{x=0.059m}}{(B_y l)_{B6}} = \begin{cases} 0.910^{-4} \text{ for the octupole} \\ 0.610^{-4} \text{ for the dodecapole} \end{cases}$$

These values are comparable to those found for the main dipoles (Table 2.1).

2.5 Dispersion suppressor and straight section quadrupoles

Table 2.6 gives at 20GeV and 45GeV (before β-squeezing) the integrated gradient errors at the aperture of 0.059m for all MQA type quadrupoles i.e. QS, L1 and QS,L3 to QS,L18 (QS,L2 made of two MQ type quadrupoles is not included). At a given energy they have different currents but the range is small enough so that only one set of multipole errors can be defined for all the quadrupoles.

Most of the quadrupoles have aluminium chambers with a nickel layer which perturbs the field distribution, in particular the octupole and dodecapole components. The reduction of the quadrupole strength has been taken into account in the excitation curves used for operation. The quadrupoles listed in Table 2.7 have stainless steel vacuum chamber without "nickel effect". For the quadrupole circuits QL3 and QL4 of Point 1, only one of the two quadrupoles which are in series has an aluminium chamber; for these two circuits only half of the gradient reduction due to nickel was corrected in the Gl/I tables used in LEP operation.

2.6 Sextupoles

The excitation currents of the sextupoles are the following:
at 20GeV:

SF1 = 4.1A SD1 = 6.2A
SF2 = 8.3A SD2 = 4.7A
SF3 = 10.1A SD3 = 6.1A

at 45 GeV before β squeezing:

SF1 = 18A SD1 = 15.9A
SF2 = 17.7A SD2 = 12.7A
SF3 = 21.6A SD3 = 15.7A

while the sextupoles have been designed for a maximum current of 360A.

At these very low excitation levels, the dispersion between magnets and the multipole content (mainly the 10 pole component) depends very much on the actual current. Table 2.8 gives the errors for the magnets themselves expressed as the relative integrated sextupole error at the aperture limit of 0.059m. It should be noted that the multipole content has been measured on the whole production at 18A and above only; the systematic components given for lower currents have been calculated by adding the variation of the components subsequently measured on one SF and one

SD sextupole to the 18A values; the dispersion of the 10 pole component has been increased in the same ratio as the dispersion of the sextupole component.

The influence of the nickel layer has not been measured. An order of magnitude of the perturbation can be derived from comparison with the regular lattice quadrupoles: at 6A in the sextupoles, the field on the nickel layer is 8 to 17 times lower (whether one considers the height or the width of the vacuum chamber) than that produced by the quadrupole at 20GeV; since the nickel layer is saturated, the reduction of the sextupole strength will be of the order of 8 to 17 times higher than the strength reduction of the quadrupoles, i.e. between 1 and 2%. If one calculates the perturbations of the multipoles in terms of integrated field variations in the half cell, one should obtain smaller values than those found for the regular lattice quadrupoles due to the smaller lengths of the sextupoles; $\Delta Bl/Bl$ values below 0.5 10^{-4} are expected.

The perturbation due to the nearby quadrupole has not been measured. However, considering the small reverse effect (sextupole on quadrupole) and by referring again to the half cell, it is very likely that this perturbation is negligible.

2.7 Alignment in the tunnel

The alignment errors found in the overall survey performed at the end of the installation period are the following:

- short wavelengths:

  one quadrupole with respect to the adjacent ones:
  $< \Delta x >=< \Delta y >$ = 0.1mm r.m.s.

  dipoles with respect to the adjacent quadrupoles:
  $< \Delta x >=< \Delta y >$ = 0.3mm r.m.s.

- long wavelengths:

  the envelopes of the radial and vertical errors of the magnets are shown in Figures 2.1 and 2.2 respectively

- transverse tilt:

  dipoles and straight section units (quadrupole, sextupole, corrector)
  $< \Delta\theta >$ = 0.1mrad r.m.s.

- longitudinal position:

  quadrupoles $< \Delta s >$ = 1.0mm r.m.s.

  length of dipole pairs $< \Delta l >$ = 1.5mm r.m.s.

2.8 Coupling

From measurements performed with the beams using the horizontal bumps method, quadrupole and sextupole skew components of up to $B' = 2Gm^{-1}$ and $B'' = 100Gm^{-2}$ have been found [4]; the sextupole component is calculated by assuming that the coupling source in arc 4 which would otherwise correspond to a gradient of the order of $1Gm^{-1}$ is actually a pure sextupole producing the same field at 20mm (maximum amplitude of the applied horizontal bumps). These components which are independent of energy correspond to the $\Delta Bl/Bl$ quoted in Tables 2.1 to 2.4.

These skew fields are mainly produced by the initial magnetization of the nickel layer of the dipole vacuum chambers [5]; the magnetic measurements performed on samples of vacuum chambers have shown large variations: the systematic error ϵ and the dispersion $< \Delta\epsilon >$ between dipole pairs

are very likely of the same order of magnitude; it was shown later in the Workshop that **such a dispersion might explain a large fraction of the abnormal vertical dispersion.** The other main sources of coupling are the asymmetry of the dipole excitation bars and the residual earth field in the dipole gap. The positions of the inner bars which are the most critical have been measured in the tunnel, at the ends of each dipole core: the resulting quadrupole and sextupole skew terms are given in Table 2.1. The contributions to coupling of the bars and residual earth field are shown in Figures 2.3 and 2.4. These contributions will predominate after demagnetisation of the vacuum chambers (shutdown 1991-1992).

It is, therefore, important to pursue the programme of coupling measurements with the π bump method around the ring; the a priori knowledge of the phase of the perturbation should be more fully exploited to determine the local quadrupole and sextupole components. A cycle type measurement with a 1 minute or so repetition time (orbit measurement - bump applied - orbit measurement - bump suppressed) might also be envisaged to improve the precision. **The correlation of the residual coupling in the demagnetised sections with the position of the excitation bars will indicate if a more precise fitting of the bars should be done together with the demagnetisation.**

References

[1] J. Billan, J.P. Gourber, G. Guignard, K. Henrichsen, J. Mangain and R. Wolf, Magnetic Performance of the LEP bending magnets, Proceedings of the 1989 IEEE Particle Accelerator Conference, Chicago.

[2] V. Remondino, T. Verbeeck, L. Walkiers, R. Wolf and C. Wyss, Design manufacture and performance of LEP magnetic lenses, IEEE Trans. on Magnetics, Vol 24, No. 2, March 1988, pp 1342-1345

[3] G. Guignard, Tolerances for the magnetic elements of the LEP lattice, Proceedings of the 12th International Conference on High Energy Accelerators, Fermilab 1983

[4] LEP Commissioning Notes 17, 18, 25 and 40

[5] J. Billan, Coupling of transverse movements in LEP, or what 7μm of nickel can really do, CERN/AC seminar, 3rd December 1990

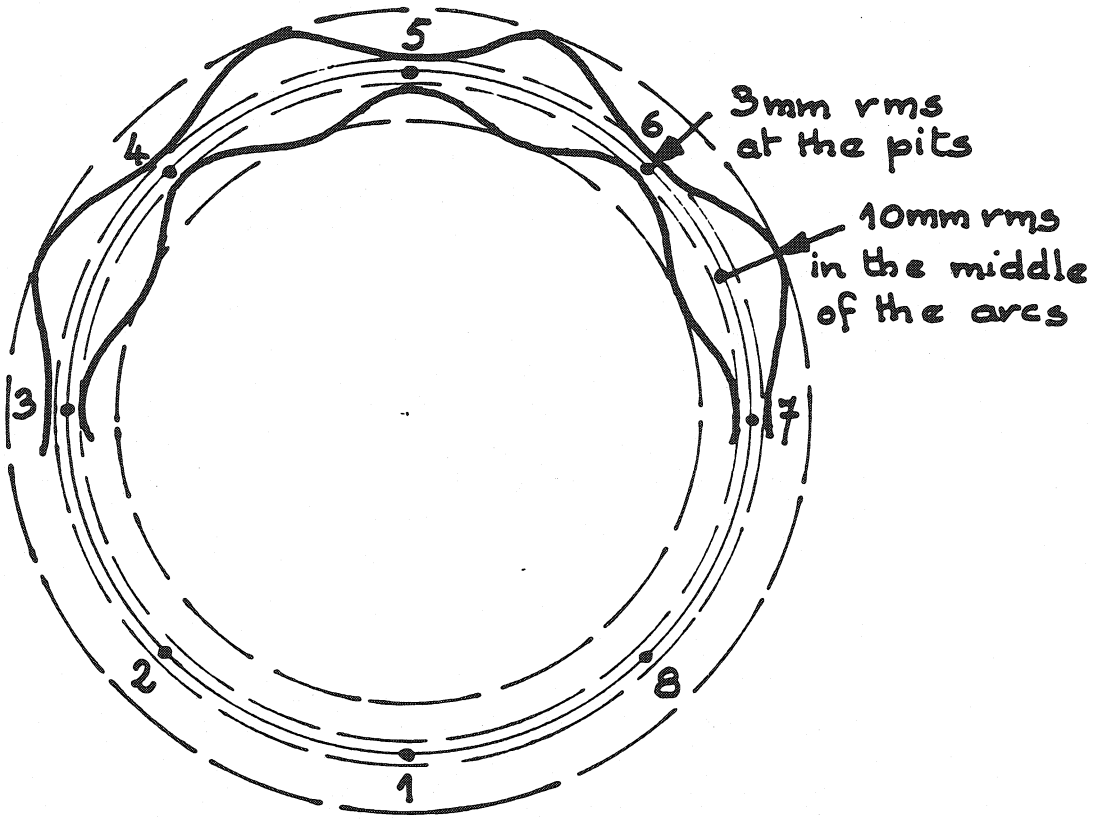

Figure 2.1: Long wavelength radial alignment errors

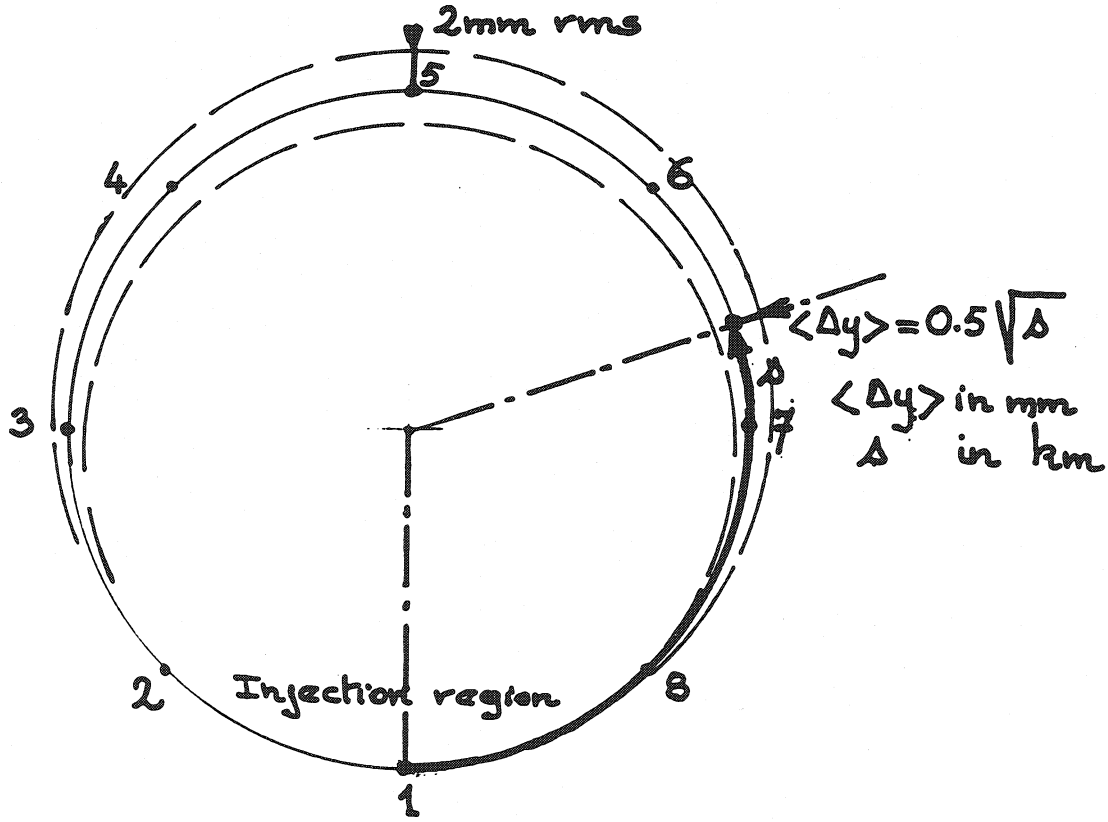

Figure 2.2: Long wavelength vertical alignment errors

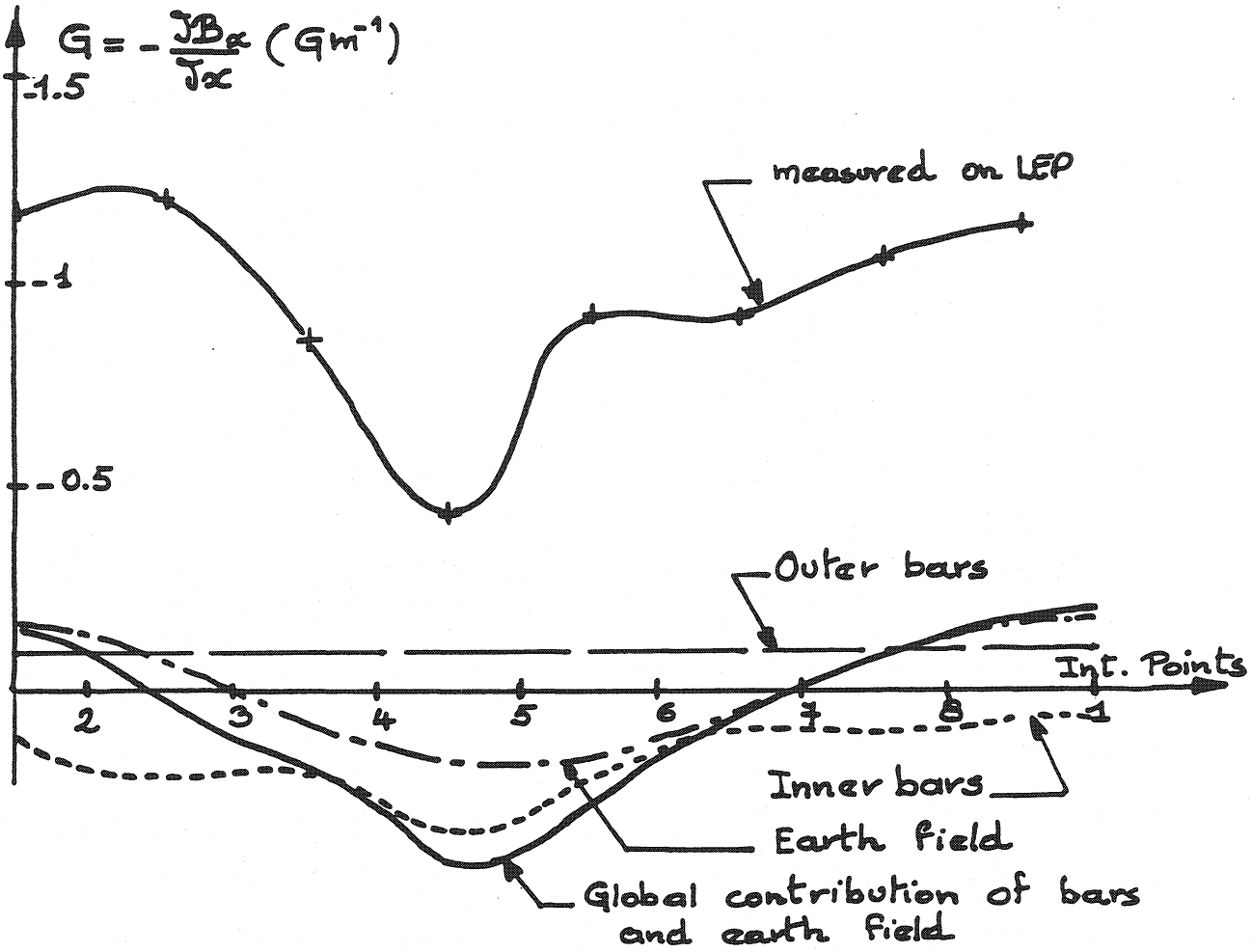

Figure 2.3: Coupling at 20 GeV

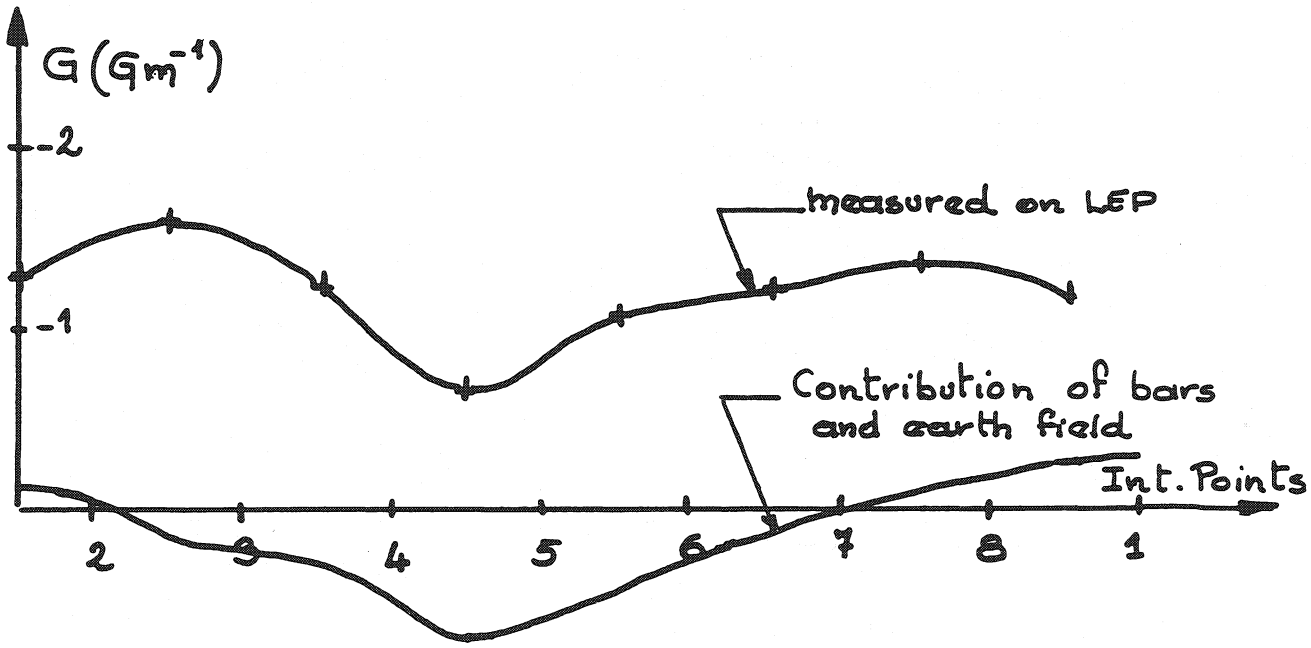

Figure 2.4: Coupling at 45.5 GeV

Table 2.1

Field errors in the main dipole pairs (in units of 10^{-4})

COMPONENTS		TOLERANCES		20 GeV							45 GeV						
				Magnet*		Vac.chamber		Alig.	Global		Magnet*		Vac.chamber		Alig.	Global	
		e	<Δe>	e	<Δe>	e	<Δe>	<Δe>	e	<Δe>	e	<Δe>	e	<Δe>	<Δe>	e	<Δe>
Normal	2 p.	-	-	-	<7	$-7.4^{\pm}$	0.7	1.5	-	<7	-	<7	$-5.8^{\pm}$	0.6	1.5	-	<7
Skew	2 p.	-	-	0.0	0.5	-	-	1.0	0.0	1.1	0.0	0.5	-	-	1.0	0.0	1.1
Normal	4 p.	±8	1.4	-0.8	0.7	$-8^{\pm}$	0.7	-	$-8.8^{\pm}$	1.0	0.0	0.8	$-3.7^{\pm}$	0.3	-	$-3.7^{\pm}$	0.9
Skew	4 p.	-	-	0.3	0.9	up to	5	-	up to	5	0.3	0.9	up to	2	-	up to	2
Normal	6 p.	+2/-5	2.0	-4.8	0.6	$4^{\pm}$	0.4	-	$-0.8^{\pm}$	0.7	-3.3	0.6	$1.8^{\pm}$	0.2	-	$-1.5^{\pm}$	0.6
Skew	6 p.	-	-	1.1	0.5	up to	8	-	up to	8	1.1	0.5	up to	4	-	up to	4
Normal	8 p.	±0.7	1.4	-3.4	0.3	$3.9^{\pm}$	0.3	-	$0.5^{\pm}$	0.4	-1.9	0.2	$1.7^{\pm}$	0.2	-	$-0.2^{\pm}$	0.3
Skew	8 p.	-	-	-	-	-	-	-	-	-	-	-	-	-	-	-	-
Normal	10 p.	±1.8	1.4	2.6	0.7	$-3.2^{\pm}$	0.4	-	$0.6^{\pm}$	0.8	1.4	0.6	-1.4	0.1	-	$0.0^{\pm}$	0.6

*including shims

Table 2.2

Field errors in the low field dipole pairs (in units of 10^{-4})

COMPONENTS		TOLERANCES		20 GeV							45 GeV						
				Magnet		Vac.chamber		Alig.	Global		Magnet		Vac.chamber		Alig.	Global	
		e	<Δe>	e	<Δe>	e	<Δe>	<Δe>	e	<Δe>	e	<Δe>	e	<Δe>	<Δe>	e	<Δe>
Normal	2p.	-	-	-	4.3	$-7.4^{\pm}$	0.7	1.5	-	4.6	-	1.5	$-5.5^{\pm}$	0.6	1.5	-	2.2
Skew	2 p.	-	-	0.0	0.5	-	-	1.0	0.0	1.1	0.0	0.5	-	-	1.0	0.0	1.1
Normal	4 p.	±8	1.4	-3.2	-	$-8^{\pm}$	0.7	-	$-11.2^{\pm}$	-	-0.6	-	$-3.7^{\pm}$	0.3	-	$-4.3^{\pm}$	-
Skew	4 p.	-	-	0.0	-	up to	5	-	up to	5	0.0	-	up to	2	-	up to	2
Normal	6 p.	+2/-5	2.0	-0.5	-	$4^{\pm}$	0.4	-	$3.5^{\pm}$	-	-0.2	-	$1.8^{\pm}$	0.2	-	$1.6^{\pm}$	-
Skew	6 p.	-	-	-	-	up to	8	-	up to	8	-	-	up to	4	-	up to	4
Normal	8 p.	±0.7	1.4	0.0	-	$3.9^{\pm}$	0.3	-	$3.9^{\pm}$	-	0.0	-	$1.7^{\pm}$	0.2	-	$1.7^{\pm}$	-
Skew	8 p.	-	-	-	-	-	-	-	-	-	-	-	-	-	-	-	-
Normal	10 p.	±1.8	1.4	0.0	-	$-3.2^{\pm}$	0.4	-	$-3.2^{\pm}$	-	0.0	-	-1.4	0.1	-	$-1.4^{\pm}$	-

Table 2.3

Field errors in the returned dipole pairs (in units of 10^{-4})

COMPONENTS		TOLERANCES		20 GeV Magnet* e	20 GeV Magnet* <Δe>	20 GeV Vac.chamber e	20 GeV Vac.chamber <Δe>	20 GeV Alig. <Δe>	20 GeV Global e	20 GeV Global <Δe>	45 GeV Magnet* e	45 GeV Magnet* <Δe>	45 GeV Vac.chamber e	45 GeV Vac.chamber <Δe>	45 GeV Alig. <Δe>	45 GeV Global e	45 GeV Global <Δe>
		e	<Δe>														
Normal	2 p.	-	-	-	<7	$-7.4^{\pm}$	0.7	1.5	-	<7	-	<7	$-5.8^{\pm}$	0.6	1.5	-	<7
Skew	2 p.	-	-	0.0	0.5	-	-	1.0	0.0	1.1	0.0	0.5	-	-	1.0	0.0	1.1
Normal	4 p.	±8	1.4	7.2	0.7	$-8^{\pm}$	0.7	-	$-0.8^{\pm}$	1.0	-4.1	0.8	$-3.7^{\pm}$	0.3	-	$-7.8^{\pm}$	0.9
Skew	4 p.	-	-	-	-	up to	5	-	up to	5	-	-	up to	2	-	up to	2
Normal	6 p.	+2/-5	2.0	-4.8	0.6	$4^{\pm}$	0.4	-	$-0.8^{\pm}$	0.7	-2.9	0.6	$1.8^{\pm}$	0.2	-	$-1.1^{\pm}$	0.6
Skew	6 p.	-	-	-	-	up to	8	-	up to	8	-	-	up to	4	-	up to	4
Normal	8 p.	±0.7	1.4	-2.8	0.3	$3.9^{\pm}$	0.3	-	$1.1^{\pm}$	0.4	-1.9	0.2	$1.7^{\pm}$	0.2	-	$-0.2^{\pm}$	0.3
Skew	8 p.	-	-	-	-	-	-	-	-	-	-	-	-	-	-	-	-
Normal	10 p.	±1.8	1.4	2.4	0.7	$-3.2^{\pm}$	0.4	-	$-0.8^{\pm}$	0.8	-1.1	0.6	$-1.4^{\pm}$	0.1	-	$-2.5^{\pm}$	0.6

*including shims

Table 2.4

Field errors in the injection region dipoles (in units of 10^{-4})

COMPONENTS		TOLERANCES		20 GeV Magnet* e	20 GeV Magnet* <Δe>	20 GeV Vac.chamber e	20 GeV Vac.chamber <Δe>	20 GeV Alig. <Δe>	20 GeV Global e	20 GeV Global <Δe>	45 GeV Magnet* e	45 GeV Magnet* <Δe>	45 GeV Vac.chamber e	45 GeV Vac.chamber <Δe>	45 GeV Alig. <Δe>	45 GeV Global e	45 GeV Global <Δe>
		e	<Δe>														
Normal	2p.	-	-	-	<5	$-3.7^{\pm}$	0.4	0.0	-	<5	-	<6	$-2.9^{\pm}$	0.3	0.0	-	<6
Skew	2 p.	-	-	0.0	0.5	-	-	1.0	0.0	1.1	0.0	0.5	-	-	1.0	0.0	1.1
Normal	4 p.	±8	1.4	-6.4	1	$-4^{\pm}$	0.5	-	$-10.4^{\pm}$	1.1	-6.0	1.2	$-1.8^{\pm}$	0.2	-	$-7.8^{\pm}$	1.2
Skew	4 p.	-	-	-	-	up to	3	-	up to	3	-	-	up to	1	-	up to	1
Normal	6 p.	+2/-5	2.0	-2.5	0.9	$2^{\pm}$	0.3	-	$-0.5^{\pm}$	1.0	-2.0	1.0	$0.9^{\pm}$	0.2	-	$-1.1^{\pm}$	1.0
Skew	6 p.	-	-	-	-	up to	4	-	up to	4	-	-	up to	2	-	up to	2
Normal	8 p.	±0.7	1.4	-1.7	0.4	$1.9^{\pm}$	0.2	-	$0.2^{\pm}$	0.4	-1.0	0.4	$0.8^{\pm}$	0.2	-	$-0.2^{\pm}$	0.5
Skew	8 p.	-	-	-	-	-	-	-	-	-	-	-	-	-	-	-	-
Normal	10 p.	±1.8	1.4	-0.9	1.0	$-1.6^{\pm}$	0.3	-	$-2.5^{\pm}$	1.1	-1.8	1.2	$-0.7^{\pm}$	0.1	-	$-2.5^{\pm}$	1.2

*including shims

Table 2.5

Gradient errors in the regular lattice quadrupoles (in units of 10^{-4})

COMPONENTS		TOLERANCES		20 GeV - I = 57 A							45 GeV - I = 128 A						
				Magnet*		Vac.chamber		Alig.	Global		Magnet*		Vac.chamber		Alig.	Global	
		e	<Δe>	e	<Δe>	e	<Δe>	<Δe>	e	<Δe>	e	<Δe>	e	<Δe>	<Δe>	e	<Δe>
Normal	4p.	-	-	-	4.0	$-8.0^{\pm}$	0.9	-	-	4.1	-	3.0	$-3.5^{\pm}$	0.4	-	-	3.0
Skew	4p.	-	-	0.0	0.2	-	-	2.0	0.0	2.0	0.0	0.2	-	-	2.0	0.0	2.0
Normal	6p.	6	12	-0.1	1.6	-	-	-	-0.1	1.6	-0.2	1.6	-	-	-	-0.2	1.6
Skew	6p.	6	12	-0.2	2.1	-	-	-	-0.2	2.1	0.0	1.9	-	-	-	-	-
Normal	8p.	5	10	-1.9	2.5	$35^{\pm}$	3.8	-	$33.1^{\pm}$	4.5	1.0	2.4	$15^{\pm}$	1.6	-	$16.8^{\pm}$	2.6
Skew	8p.	5	10	1.0	1.3	-	-	-	1.0	1.3	1.0	1.1	-	-	-	1.0	1.1
Normal	12p.	10	10	10.1	1.6	$-50^{\pm}$	5.5	-	$-39.9^{\pm}$	5.7	11.3	1.6	$-22^{\pm}$	2.5	-	$-10.7^{\pm}$	3.0
Normal	20p.	-	-	-3.3	1.1	-	-	-	-3.3	1.1	-3.8	1.0	-	-	-	-3.8	1.0

*including the perturbation of the nearby sextupole

Table 2.6

Gradient errors in the MQA type quadrupoles (in units of 10^{-4})

COMPONENTS		TOLERANCES		20 GeV - I ~ 30 to 60 A							45 GeV - I ~ 70 to 135 A						
				Magnet		Vac.chamber		Alig.	Global		Magnet		Vac.chamber		Alig.	Global	
		e	<Δe>	e	<Δe>	e	<Δe>	<Δe>	e	<Δe>	e	<Δe>	e	<Δe>	<Δe>	e	<Δe>
Normal	4p.	-	-	-	-	$5^{\pm}$	0.6	-	-	-	-	-	$2.2^{\pm}$	0.3	-	-	-
Skew	4p.	-	-	0.0	0.2	-	-	2.0	0.0	2.0	0.0	0.2	-	-	2.0	0.0	2.0
Normal	6p.	6	15	-2.0	2.8	-	-	-	-2.0	2.8	-1.5	2.8	-	-	-	-1.5	2.8
Skew	6p.	6	15	-1.7	3.7	-	-	-	-1.7	3.7	-0.6	3.5	-	-	-	-0.6	3.5
Normal	8p.	7.5	15	-0.7	3.8	$22^{\pm}$	2.5	-	$21.3^{\pm}$	4.5	-0.9	3.6	$10^{\pm}$	1.1	-	$9.1^{\pm}$	3.8
Skew	8p.	7.5	15	-0.0	1.7	-	-	-	0.0	1.7	0.4	1.0	-	-	-	0.4	1.0
Normal	12 p.	15	15	8.9	1.9	$-32^{\pm}$	3.5	-	$-23.1^{\pm}$	4.0	10.7	1.9	$-14^{\pm}$	1.6	-	$-3.3^{\pm}$	2.5
Normal	20p.	-	-	-2.5	3.0	-	-	-	-2.5	3.0	-2.9	2.9	-	-	-	-2.9	2.9

Table 2.7

MQA type quadrupoles with stainless steel vacuum chambers

QS1	Points 2, 4, 6, 8
QS2	Points 2, 4, 6, 8
QS3	Points 2, 4, 6, 8
QS4	Points 2, 4, 6, 8
QS7/9	Points 2, 6
QS8/10	Points 2, 6
QL3	Point 1 only 1 quad (DC 147)
QL4	Point 1 only 1 quad (DC 146)

Table 2.8

$\Delta B''l$ (x = 0.059m)/$B''l$ errors in the sextupoles (in units of 10^{-3})

COMPONENTS		TOLERANCES		MSF sextupoles						MSD sextupoles					
				I = 5.4 A		I = 10.8 A		I = 18 A		I = 3.6 A		I = 7.2 A		I = 18 A	
		e	<Δe>	e	<Δe>	e	<Δe>	e	<Δe>	e	<Δe>	e	<Δe>	e	<Δe>
Normal	6 p.	-	-	-	<5.5	-	<1.9	-	<0.7	-	<5.0	-	<2.5	-	<0.7
Skew	6p.	-	-	-	0.5	0.0	0.5	00	0.5	0.0	0.5	0.0	0.5	0.0	0.5
Normal	8p.	1.7	20	-0.1	0.8	0.0	0.8	0.2	0.8	0.1	1.0	0.0	1.1	0.0	1.0
Skew	8 p.	1.7	20	-0.8	1.4	-0.8	1.4	-1.0	1.4	-1.5	1.2	-1.2	1.2	-1.2	1.2
Normal	10 p.	3.4	20	-2.9	11	-2.2	4	-1.7	1.5	-2.1	11	-1.5	5	-1.2	1.6
Skew	10p.	3.4	20	-0.1	1.2	0.1	1.2	-0.2	1.2	0.0	1.7	0.1	1.7	0.2	1.7
Normal	18p.	16	20	1.6	0.7	1.7	0.7	2.0	0.7	-0.4	0.6	-0.1	0.6	0.0	0.6
Normal	30 p.	-	-	-2.7	0.3	-2.7	0.3	-2.7	0.3	-1.7	0.4	-1.8	0.4	-1.8	0.4